DOI: 10.1177/1468087414564230 Pre-Print

Effect of hydrogen peroxide addition to methane fueled homogeneous charge compression ignition engines through numerical simulations

Zachary M. Hammond[a,b], J. Hunter Mack[a], and Robert W. Dibble[a]

[a] University of California Berkeley, Berkeley, California, United States
[b] Corresponding Author: Email: zmh@berkeley.edu

Abstract

The effect of the direct injection of hydrogen peroxide into a port-injected methane fueled homogeneous charge compression ignition engine was investigated numerically. The injection of aqueous hydrogen peroxide was implemented as a means of combustion phasing control. A single cylinder homogeneous charge compression ignition engine (2.43 L Caterpillar) was modeled using the Cantera 2.0 flame code toolkit, the GRI-Mech 3.0 chemical reaction mechanism, and a single-zone slider-crank engine model. Start of injection timing and the amount of injected hydrogen peroxide were manipulated to achieve desired combustion phasing under a wide range of intake temperatures. As the concentration of hydrogen peroxide is increased, the combustion phasing is advanced up to 22 degrees for the conditions investigated in this study. This advancing effect is most pronounced at small concentrations (< 10 g H_2O_2 / kg CH_4) and early injection timings (SOI < 25 degrees BTDC). The model suggests hydrogen peroxide can be introduced as a means of combustion phasing control while maintaining the low emissions and peak in-cylinder pressures inherent in homogeneous charge compression ignition engines.

Keywords

Homogeneous charge compression ignition, methane, hydrogen peroxide, dual fuel, autoignition, modeling, single-zone model, combustion phasing control

Published in the International Journal of Engine Research, Vol 17, Issue 2, pp. 209-220, 2016
DOI: 10.1177/1468087414564230

Introduction

Homogeneous Charge Compression Ignition (HCCI) has proven to be an attractive internal combustion technique in attaining low emissions and high fuel efficiency.[1] However, the dependence on auto-ignition through chemical kinetics creates difficulty in attaining a controlled ignition event, especially over a wide range of intake conditions.[2] Techniques for controlling the ignition event include managing the intake temperature through resistance heating of the intake air,[3,4] variable valve actuation,[5] and exhaust gas recirculation.[6] Another promising approach to controlling combustion timing in HCCI uses two fuels to drive combustion.[7-11] In this dual-fuel strategy, the difference in the combustion characteristics of each fuel is exploited to regulate the reactivity of the in-cylinder charge.[12] Dual fuel strategies can either combine fuels as a premixed charge or through in-cylinder injection of a secondary fuel. This study proposes that hydrogen peroxide (H_2O_2) may be a suitable additive to introduce through direct injection as a means of control.

Due to its role as a critical oxidizer in the initiation of thermal ignition, H_2O_2 concentration is a main determinant of the rate of heat release.[13] It has also been shown to increase gross indicated mean effective pressure (IMEP) and advance ignition timing.[14] Therefore, the manipulation of the concentration of H_2O_2 may allow for the control of the combustion event. It is also worth noting that H_2O_2 is both inexpensive and readily available, thus making it a practical and economical choice as an additive. In application, use of the aqueous H_2O_2 mixture for combustion timing would not be implemented for every cycle – only to overcome changes in operating conditions to maintain the engine at optimal combustion phasing. For a natural gas vehicle with a 10 GGE (Gasoline Gallon Equivalent) tank at an extreme case of secondary injection occurring at 10% of all cycles using a 1% H_2O_2 solution, the total consumption of the aqueous mixture would be 0.68 gallons.

Previous studies have shown that pre-mixed fuels of H_2O_2 in methane have drastically reduced the intake temperature required to achieve ignition at a given crank angle degree (CAD).[15] The same findings were seen in engines running a mixture of H_20_2 and ethanol.[16] However, the use of H_20_2 has not been investigated as a cycle-to-cycle controlling device; only as a combustion enhancer for pre-mixed fuels.

In order to take advantage of the beneficial characteristics of H_2O_2 addition seen by other investigators, the authors employed H_2O_2 as a means of control by studying the effects of directly injecting an aqueous H_2O_2 solution into the combustion chamber of an HCCI engine through numerical simulations.

Additionally, as H_2O_2 is typically transported in an aqueous mixture due to safety concerns, there will also be a significant amount of water introduced in the process of direct injecting the secondary fuel. Addition of water in HCCI engines has been shown to reduce peak in-cylinder temperatures; resulting in lower NO_x emissions but an increase in HC and CO emissions.[17-20] Previous research on pilot injection of a secondary fuel into an engine running primarily on premixed fuel has shown the approach to be effective and cost effective.[21-23] Additional considerations regarding the inclusion of an aqueous H_2O_2 mixture might affect component selection so as to avoid material degradation, though previous studies using water injection strategies have not found it prohibitive.[17-20] The accompanying water may also have negative effects on the emissions of CO and unburned hydrocarbons.[17] Furthermore, water injection may cause problems with operation or storage of the engine at sub-zero temperatures.

Objective and approach

A single-zone model was used to investigate the effect of H_2O_2 addition through direct injection into a pre-mixed charge of methane in air. Parameters varied in the simulations include the start of injection (SOI), the intake temperature (T_{in}), and the amount of H_2O_2. In all trials, the injected liquid is an aqueous mixture of H_2O_2 at a concentration of one percent by mass. This concentration was chosen for two reasons. First, this concentration is considered a stable mixture and a safe means of transporting H_2O_2 in close proximity to a heat source. According to the United States Department of Labor's Occupational Safety and Health Administration, H_2O_2 in concentrations above eight percent by mass is a potential fire or explosion hazard.[24] Secondly, the total volume of aqueous H_2O_2 introduced during the direct injection event is similar to amounts introduced in experimental studies which directly injected water[18] and light naptha.[25] The amount of the aqueous H_20_2 mixture introduced in the simulations ranges from 0-0.3g/cycle. While this amount is significantly lower than in an engine where all the fuel is directly injected into the cylinder, it falls within an acceptable range for a direct injection system.[18]

Expanding on the analysis of the repercussions of the pure water accompanying the H_2O_2, Figure 1 displays pressure profiles with injections of varying concentrations of the aqueous H_2O_2 mixture. The mass of H_2O_2 was held constant at 0.5 mg for each of the four simulations in this figure, and the mass of the water was changed to achieve each concentration. An intake temperature of 440 K was used for these simulations. Combustion phasing is advanced as the H_2O_2 concentration is increased. There are shortcomings of an unnecessarily low H_2O_2 concentration, as the effects of

the accompanying water oppose the effects of the H_2O_2. A diluted mixture requires a larger volume of injection thereby reducing the fuel efficiency. Conversely, enough water needs to be added to ensure the volume of the injection is sufficiently large to ensure proper functionality of the fuel injector. Additionally, low H_2O_2 concentration may limit part degradation.

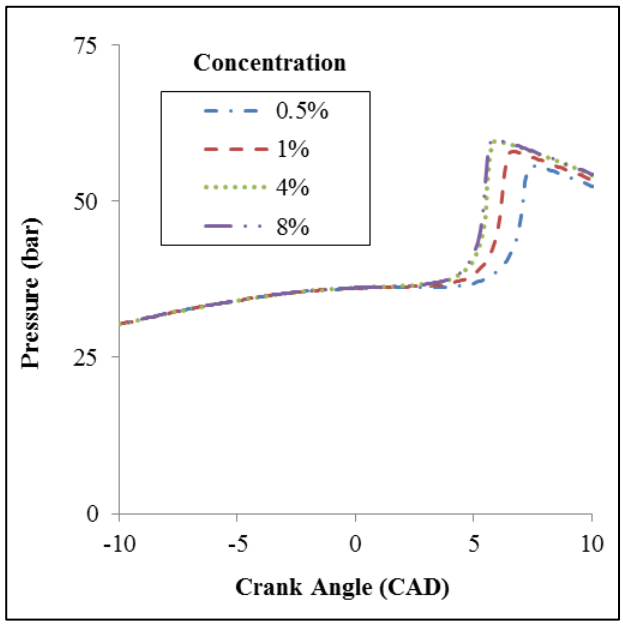

Figure 1. The effects on the temperature profile created by equivalent injections of pure water and aqueous H_2O_2 have on CA50 when SOI is -5 CAD and the intake temperature is 460 K.

Large quantities of the solution can alter the heat capacity ratio bringing concomitant thermal property changes in addition to the chemical effects. Figure 2 presents the heat capacity ratio as a function of the mass of injection. Gamma in Figure 2 was determined by adding H_2O_2 and water to a methane and air gas mixture with an equivalence ratio of 0.3. The heat capacity ratio tends towards the heat capacity of steam as the mass of injection rises. This reduction in the heat capacity ratio is, in part, responsible for the reduction of peak in-cylinder temperatures with increased mass of injection. This will be discussed in more detail below.

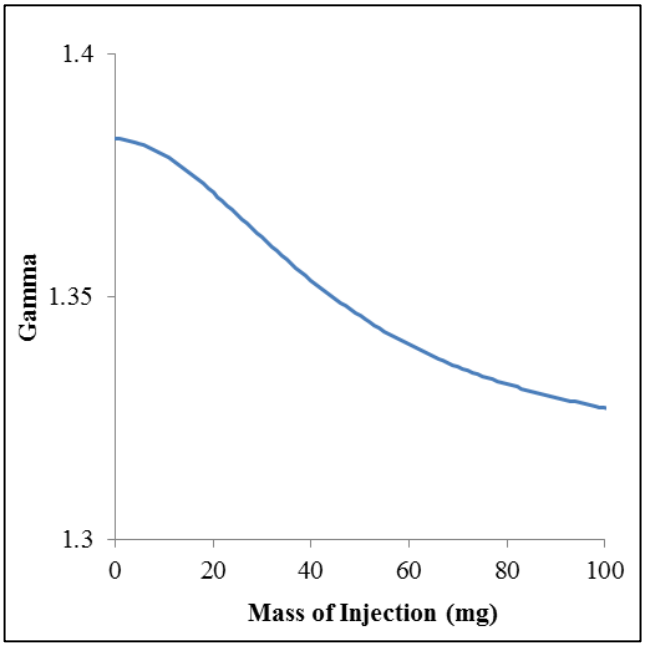

Figure 2. Heat capacity ratio as a function of the mass of injection. The concentration of the aqueous H_2O_2 mixture is 1% by mass.

Computational model

A single cylinder HCCI engine was modeled with MATLAB using the Cantera 2.0 flame code toolkit,[26] the GRI-Mech 3.0 chemical reaction mechanism,[27] and a single-zone slider-crank engine model.[28] The GRI-Mech 3.0 chemical reaction mechanism incorporates 53 species and 325 reactions. As a result of the single-zone model disregarding the subtle mass, temperature, and pressure stratifications within the cylinder, it fails in providing reliable numerical values of emissions, temperatures, and peak in-cylinder pressures. However, a single-zone model does provide for a sufficient analysis of overall combustion trends. The single-zone model provides a reasonable approximation of HCCI combustion in that the entire charge ignites nearly simultaneously throughout the cylinder without a flame front.[16] It has been shown that a single-zone model captures combustion phasing acceptably in comparison with multi-zone models.[29]

The engine modeled in these experiments is a six cylinder Caterpillar (CAT) 3406 modified for HCCI operation.[1] A single cylinder is modeled in the simulations. Engine parameters are included in Table 1.

Table 1. Caterpillar 3406 Engine Parameters.[1]

Configuration	6-cylinder
Total Displacement	14.6 L
Bore	137 mm
Stroke	164 mm
Compression Ratio (CR)	16:1

The single-zone model used in these simulations was validated using experimental data from the CAT 3406 engine. An ensemble average of 50 traces obtained during firing conditions using natural gas were used to tune the model.[1] The compression ratio of the single-zone model was reduced to 14 in order to reasonably match the simulated motoring trace and the experimental data. A connecting rod length of 262 mm was used in the simulation. Figure 3 shows a comparison between the experimental and numerical results. The results show that the simulation data are in relatively good agreement with the experimental results.

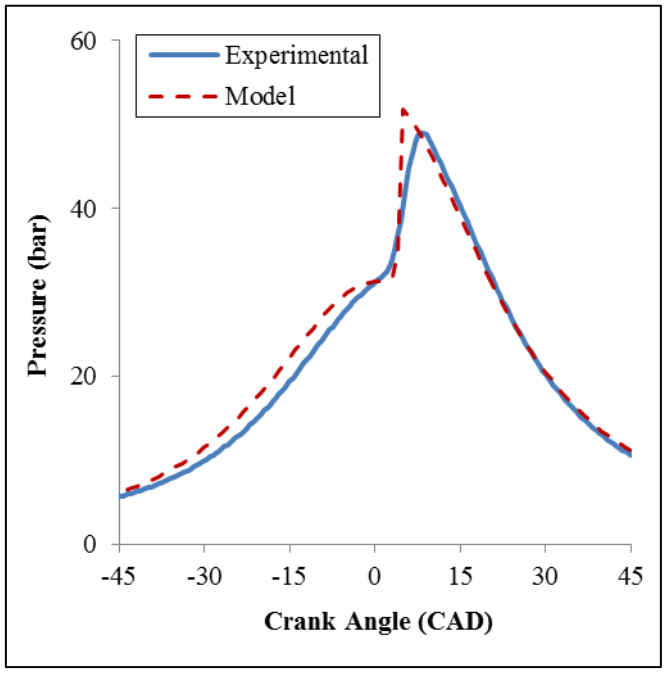

Figure 3. Comparison of the in-cylinder pressure for experimental and numerical data.

The simulation occurs between bottom dead center (BDC) of the compression stroke and BDC of the power stroke. The injection of the H_2O_2 solution was modeled as a homogeneous addition to the combustion chamber. This solution was modeled as an aqueous mixture of one percent H_2O_2 by mass. Methane was used as the primary fuel for this simulation because it does not readily achieve auto-ignition in HCCI and exhibits increased reactivity in the presence of H_2O_2.[30] An overall equivalence ratio of 0.3 was maintained in these simulations.

The numerical simulation was performed at atmospheric intake pressure and at various intake temperatures to measure the relationships between H_2O_2 concentration, start of injection (SOI) timing, and combustion timing. Combustion timing is measured by the crank angle at which fifty percent of the total heat has been released (CA50).[28]

Results and discussion

It was found that the addition of small concentrations of H_2O_2 provided a significant advance in combustion timing. In small concentrations, H_2O_2 could induce combustion of methane under conditions that would otherwise result in a misfire. Small amounts of the aqueous H_20_2 mixture were introduced at a SOI of -5 CAD after top dead center (ATDC) to a cylinder with an intake temperature of 440 K and atmospheric intake pressure. Figure 4 shows that increased amounts of H_2O_2 can advance the combustion event, which is evident by the steep increase in pressure. This shows a large variability in the combustion timings that can be achieved simply by manipulating the H_2O_2 concentration. Additionally, it can be seen that the ability to advance combustion diminishes at higher concentrations of H_2O_2 addition.

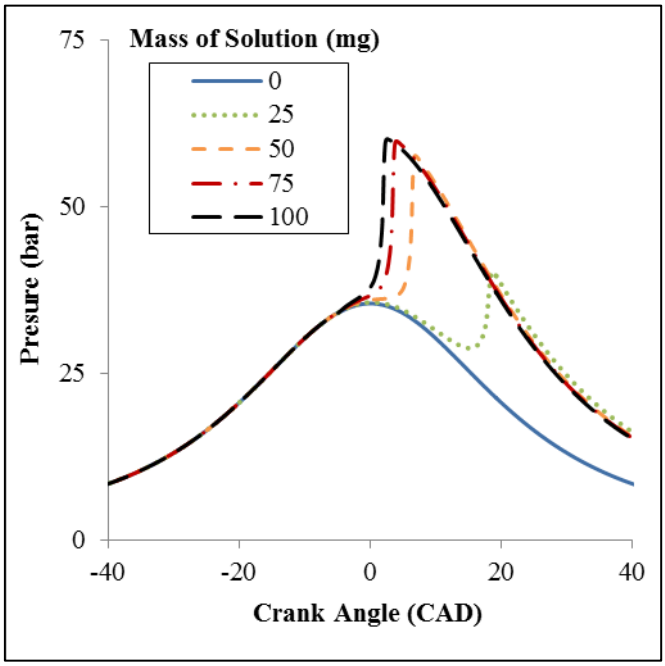

Figure 4. Effect of the quantity of injected solution on the pressure trace. Performed at an intake temperature of 440 K and a SOI of -5 CAD.

While holding intake temperature and SOI constant, varying the concentration of H_2O_2 influences combustion timing. However, the response of combustion timing to the addition of H_2O_2 exponentially decays as CA50 approaches SOI (Figure 5). At an intake temperature 450 K and a SOI of -5 CAD ATDC, concentrations of 2, 10, and 20 g H_2O_2 per kg of CH_4 achieve combustion at 33, 6, and 2 CA50 respectively. A similar effect is seen at other intake temperatures. Note that it is possible to achieve the same CA50 at a reduced intake temperature simply by increasing the concentration of H_2O_2. The intake conditions used in the simulations included in Figure 5 are such that the methane would not ignite in this HCCI engine; the addition of H_2O_2 brings the engine out of a misfire regime.

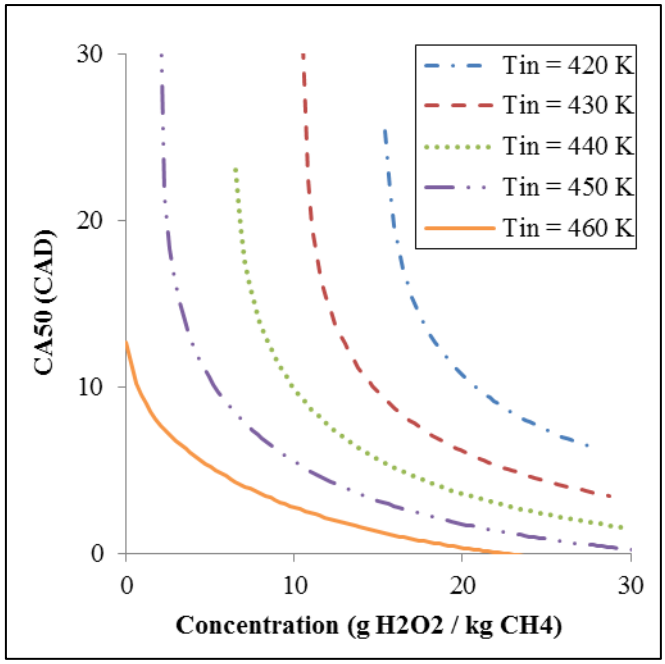

Figure 5. The relationship between the injected amount of H_2O_2 and CA50 for different temperatures when SOI is -5 CAD.

The change in CA50 shown in Figure 5 is due to the H_2O_2 in the mixture. Although the addition of water has been shown to delay combustion in HCCI, aqueous hydrogen peroxide additions can advance combustion phasing despite the low concentration of H_2O_2. Figure 6 shows a comparison between the CA50 attained when equal injections of pure water and aqueous hydrogen peroxide are directly injected at -5 SOI. Combustion is delayed as more water is introduced. Conversely, combustion is advanced as more aqueous H_2O_2 is added. Although the water accompanying the H_2O_2 may produce a cooling effect that decreases the combustion rate, the chemical effect of the H_2O_2 is significant enough to advance combustion phasing. Therefore, CA50 advances significantly when H_2O_2 is present in the secondary injection when compared to water alone.

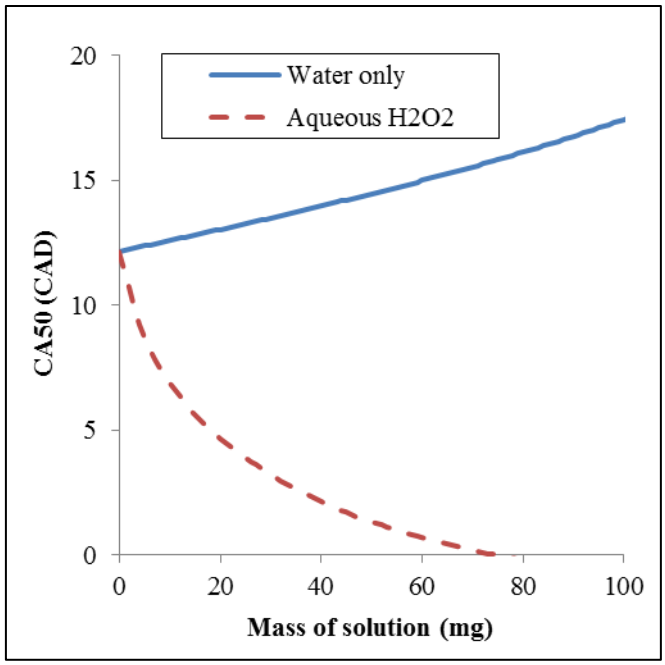

Figure 6. The effects on CA50 of injections of pure water and aqueous H_2O_2 have on CA50 when SOI is -5 CAD and the intake temperature is 460 K. The concentration of the aqueous H_2O_2 mixture is 1% by mass.

At elevated temperatures where the ignition of methane can be achieved without H_2O_2 injection, H_2O_2 can be effective in advancing CA50. This advance in CA50, referred to as ΔCA50, is the difference between the CA50 achieved without H_2O_2 injection and the CA50 achieved with H_2O_2 injection.

$$\Delta CA50 = CA50_{\,w/o\,H_2O_2} - CA50_{w/\,H_2O_2} \quad (1)$$

ΔCA50 is a useful diagnostic in determining the effectiveness of H_2O_2 addition. Figure 7 shows ΔCA50 as a function of the concentration of H_2O_2. ΔCA50 grows as the concentration of H_2O_2 rises. Again, it is observed that H_2O_2 addition has the greatest effect at lower concentrations and at lower intake temperatures.

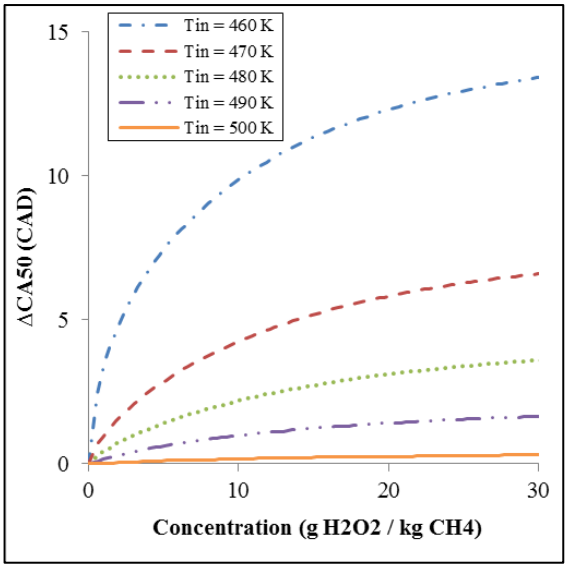

Figure 7. The relationship between the injected amount of H_2O_2 and ΔCA50 for different temperatures when SOI is -5 CAD.

To expand the range in which the injection of H_2O_2 provides a beneficial effect on combustion, injection timing was also utilized as an ignition control parameter. An advance in SOI while holding injected mass and intake temperature constant produced an advance in combustion timing. Figure 8 shows the effect of SOI changes at a constant concentration of 30 g H_2O_2 per kg CH_4 and an intake temperature of 440 K. An early SOI can be detrimental to power output if it advances CA50 before top dead center (TDC). A late SOI can marginally increase the pressure during the expansion stroke. A well timed SOI can trigger the combustion event shortly after TDC and provide for a large power output.

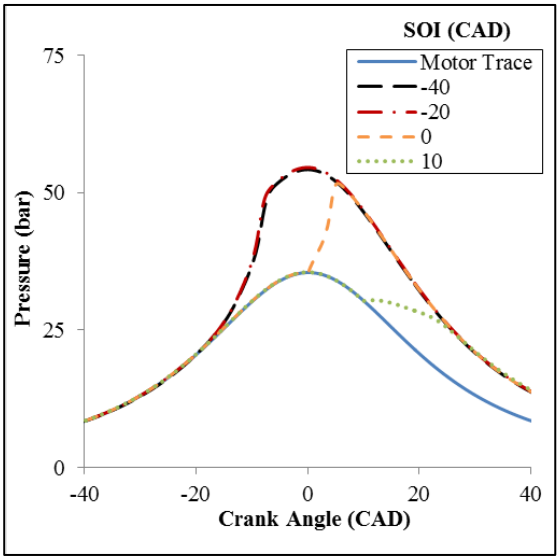

Figure 8. Effect of the start of injection on the pressure trace. Performed at an intake temperature of 440 K and a constant concentration of 30 g H_2O_2 per kg CH_4.

The relationship between SOI and CA50 has two important regimes, as shown in Figure 9. At very early SOI, a change in SOI has little effect on combustion timing. This minor effect is examined in more detailed below through an investigation of the evolution of the free radical concentration. However, as SOI increases towards a critical point, a change in SOI has an exponential effect on combustion timing. At lower temperatures this critical point demarcates the region where combustion cannot be achieved given the SOI and amount of injected solution. At higher temperatures this critical point demarcates the region where autoignition is reached before SOI (as indicated by the flat lines). The relationship between combustion phasing and SOI is seen across all intake temperatures.

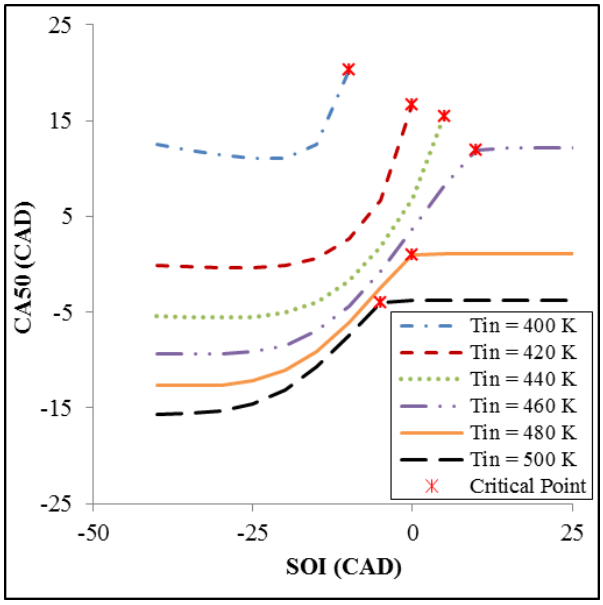

Figure 9. The relationship between the SOI of H_2O_2 and CA50 at different intake temperatures and 100 mg of injected solution.

ΔCA50 as a function of SOI at a constant injected mass of H_2O_2 is shown in Figure 10. The largest effect on combustion timing for a given injected H_2O_2 mass is seen at early SOI. The benefits of H_2O_2 addition subside as SOI is delayed until it does not affect the combustion timing at very late SOI (> 15 CAD). It is again evident that H_2O_2 addition has the greatest effect when operating at lower intake temperatures.

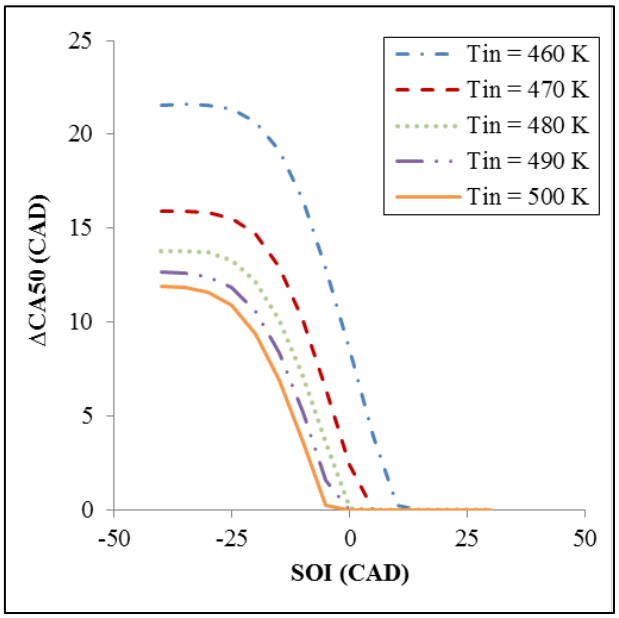

Figure 10. The relationship between the SOI of H_2O_2 and ΔCA50 at different intake temperatures and 100 mg of injected solution.

The manipulation of SOI timing in conjunction with the manipulation of H_2O_2 concentration provides two tools which can be utilized to achieve desired combustion timing under a wide range of intake conditions. A desired CA50 can be achieved with a number of different combinations of SOI and H_2O_2 concentration. Figure 11 shows a contour plot of the CA50 achieved given the SOI and H_2O_2 concentration. This simulation was conducted at atmospheric intake pressure and an intake temperature of 460 K. At these conditions, CA50 occurs at 12.1 CAD when there is no H_2O_2 injection. The slope of the contour line with respect to SOI approaches zero as SOI decreases and the slope of the contour line with respect to H_2O_2 concentration approaches zero as H_2O_2 concentration increases. However, manipulation of these parameters simultaneously provides a large range of CA50 that can be achieved.

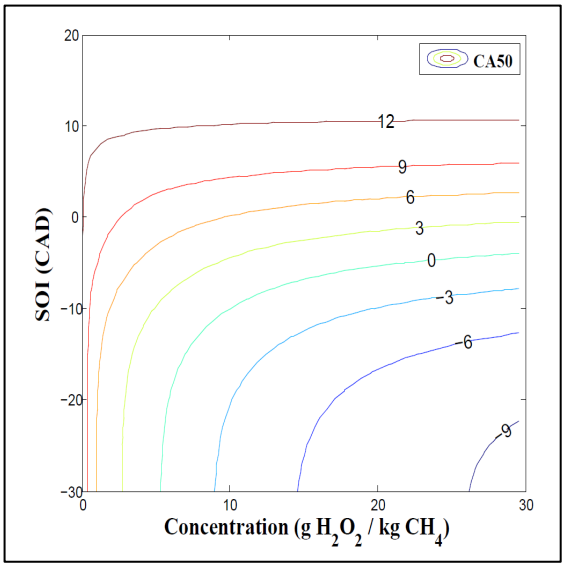

Figure 11. The combined effects of H_2O_2 concentration and SOI on CA50 at an intake temperature of 460 K.

The same data used to generate the CA50 contour plot above is used to plot the ΔCA50 contour plot in Figure 12. In this figure we can see the combined effect of SOI and H_2O_2 concentration on ΔCA50. The slope of the contour line with respect to SOI approaches zero as SOI decreases. The slope of the contour line with respect to H_2O_2 concentration approaches zero as H_2O_2 concentration increases. Once SOI is increased past the crank angle where combustion occurs in the absence of H_2O_2, ΔCA50 remains zero. ΔCA50 is advanced as SOI is advanced and H_2O_2 concentration is increased.

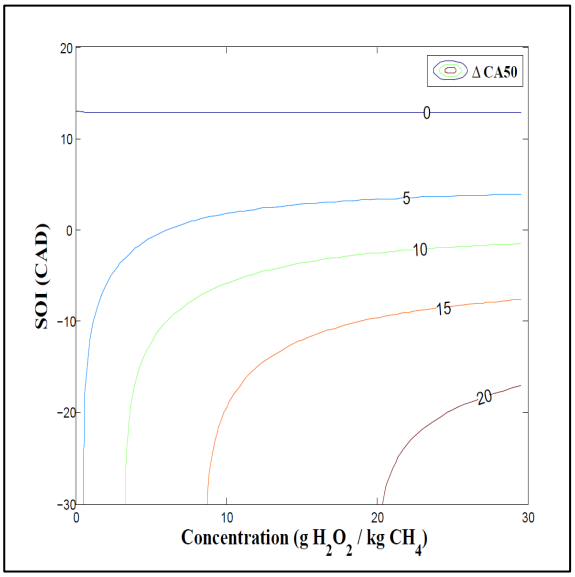

Figure 12. The combined effects of H_2O_2 concentration and SOI on the change in CA50 with respect to the CA50 achieved without H_2O_2 injection at an intake temperature of 460 K.

A detailed look at the time series evolution of key species inside the combustion chamber sheds additional light into the effect of H_2O_2 addition on the ignition process. Figure 13 shows a simulation with constant H_2O_2 addition of 100 mg, an intake temperature of 440 K, and a SOI -5 CAD. The SOI event is evident by a spike in H_2O_2 concentration. The H_2O_2 quickly dissociates into hydrogen (H), hydroxide (OH), and hydroperoxyl (HO_2) radicals. The presence of these radicals increases reactions with the methane molecules, leading towards the ignition event.

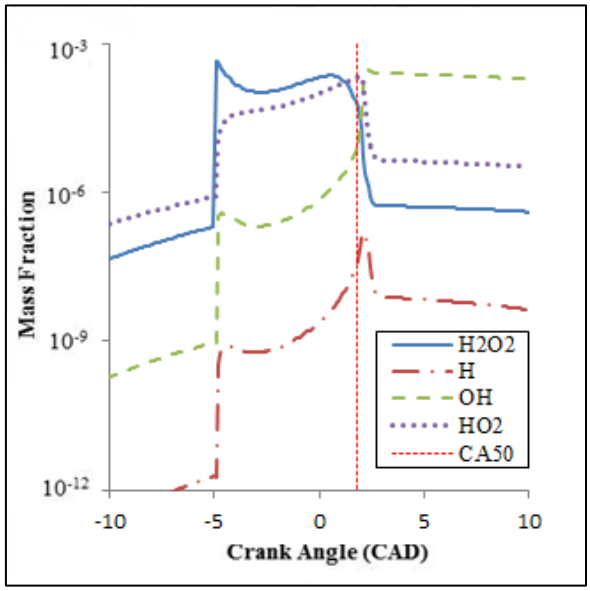

Figure 13. The evolution of four chemical species (H_2O_2, OH, H, HO_2) over time. Simulation was performed with a SOI of -5 CAD, an intake temperature of 440 K, and an injected mass of 100 mg. The vertical red line demarcates CA50.

The manipulation of the mass of the H_2O_2 addition can directly affect the concentration of free radicals. Figure 14 shows the time series evolution of the mass fraction of OH under varied injection amounts. These simulations were performed with a SOI of -5 CAD an intake temperature of 440 K. It can be seen that if enough radicals can be produced then combustion can be achieved. The radical concentrations of simulations that achieved combustion were several orders of magnitude larger the than radical concentrations of the simulations that misfired. This difference is not attributable to the difference in injected H_2O_2. Rather, if sufficient H_2O_2 is added then the radical concentration rapidly grows as the methane decomposes. Furthermore, radical concentrations of simulations that achieved combustion reached similar peak levels of radicals.

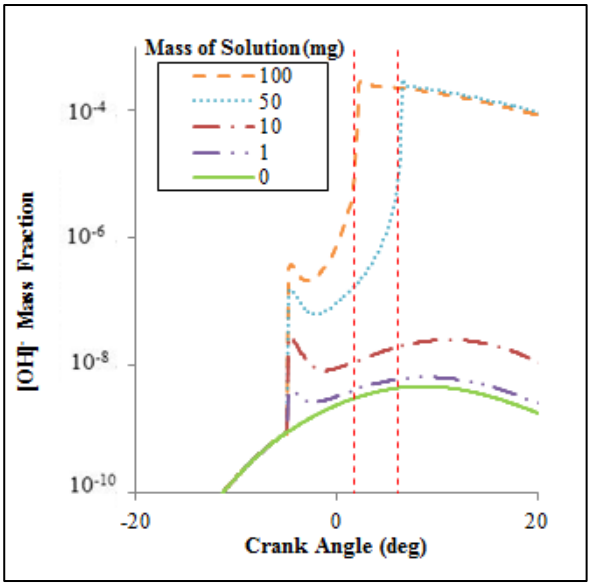

Figure 14. The effect of the amount of H_2O_2 on the evolution of hydroxide over time. Simulation was performed with and SOI of -5 CAD and an intake temperature of 440 K. The vertical red line demarcates CA50.

Additionally, the SOI of the H_2O_2 addition is a critical determinant of the time series evolution of free radicals. Figure 15 shows the time series evolution of the mass fraction of OH under varied SOI. These simulations were performed with a 100 mg injection and an intake temperature of 440 K. Advancing SOI allows the rapid growth of radicals to occur sooner. This advances CA50 in the region around TDC. However, for early SOI, the temperature is not yet high enough to trigger the combustion event soon after the injection. For these early SOI simulations, the radical concentration remains elevated until the temperature is high enough to cause rapid decomposition of methane. This results in the loss of effectiveness of early SOI.

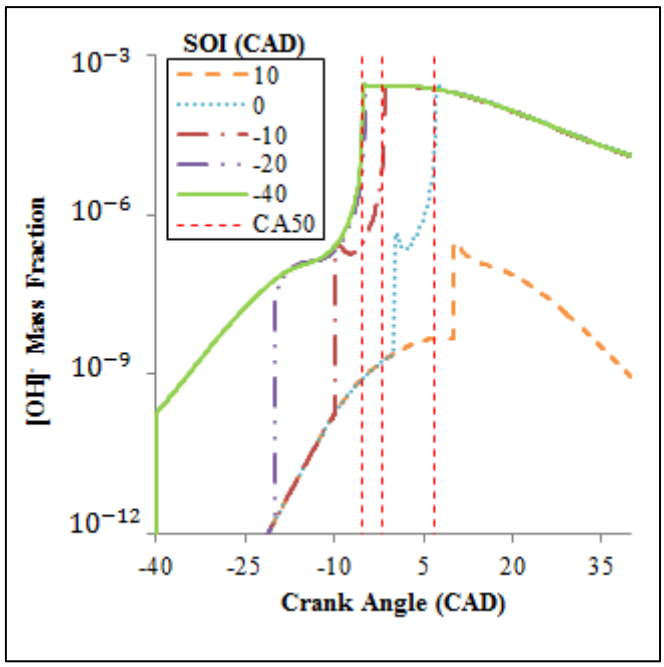

Figure 15. This Figure shows the effect of the SOI of H_2O_2 on the evolution of hydroxide over time. The vertical red line demarcates CA50.

The use of H_2O_2 as a secondary fuel in HCCI may provide control over combustion timing while retaining the benefits that make HCCI an attractive technique. In order to test the effects of H_2O_2 on pressure, temperature, and exhaust emissions, combustion timing was held constant so that the effects of H_2O_2 are isolated from the effects of combustion timing. As is the case in all single-zone engine simulations that disregard the subtle mass, temperature, and pressure stratifications within the cylinder, the values of emissions, temperatures, and peak in-cylinder pressures are most useful when viewed qualitatively with respect to the other simulations. While quantitative evaluations can be highly uncertain, the trends presented in the following figures are important in understanding the impact of H_2O_2 injection on the in-cylinder combustion process. First, the simulations suggest that H_2O_2 injection does not have significant repercussions on peak pressures within the cylinder; an important consideration since high peak pressures can damage the engine.[31] Figure 16 exhibits the effect of H_2O_2 concentration on peak pressure. SOI was adjusted to achieve a CA50 of 3 $\pm$ 0.3 CAD for all simulations. As the concentration of H_2O_2 increases, the peak in-cylinder pressure slightly decreases. Notwithstanding the over-prediction of the quantitative peak pressure results produced by the single-zone model, the qualitative trend produced by the model bolsters the notion that the H_2O_2 direct injection strategy should be explored more rigorously.

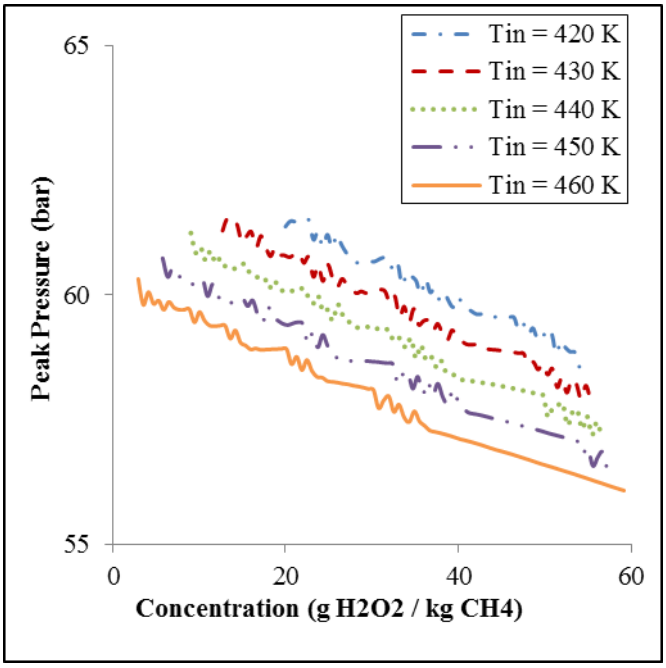

Figure 16. The relationship between the concentration of H_2O_2 and peak in-cylinder pressures while CA50 is held constant at 3 ± 0.3 CAD.

The reduction of peak in-cylinder pressure presented above is likely a ramification of decreasing in-cylinder temperatures. Figure 17 exhibits the effect of H_2O_2 concentration on peak temperature. SOI was adjusted to achieve a CA50 of 3 ± 0.3 CAD for all simulations. As more aqueous H_2O_2 is introduced, the mean specific heat increases and the gas mixture becomes more resistant to temperature change. Therefore, the peak temperature declines as the concentration of H_2O_2 is raised.

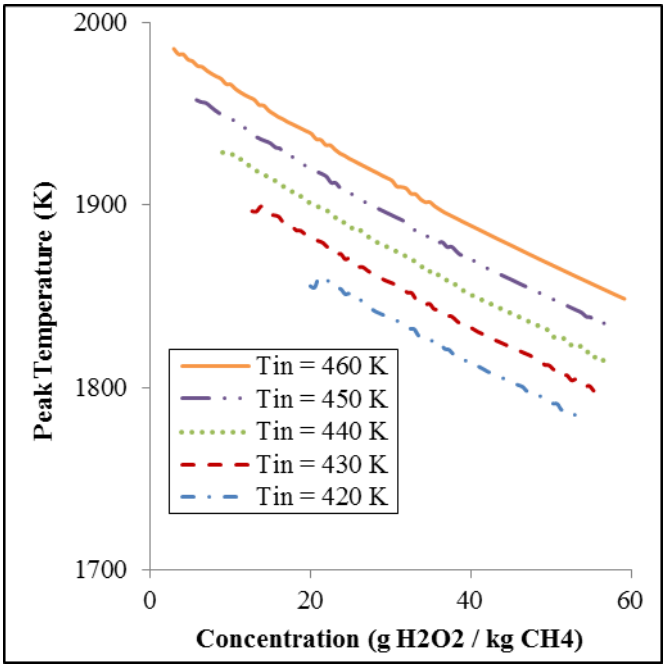

Figure 17. The relationship between the concentration of H_2O_2 and peak in-cylinder temperatures while CA50 is held constant at 3 ± 0.3 CAD.

Figure 18 presents these trends from another perspective. In this figure, the temperature profile is seen over CAD for five different cases. First, the figure includes the temperature profile of a cycle with no injection with an intake temperature of 460 K. The temperature profile of a small injection (10 g H2O2 / kg CH4) of aqueous H2O2 was

plotted as well as the temperature profile for a mass equivalent injection of pure water. Finally, the temperature profiles were plotted for a large injection (30 g H2O2 / kg CH4) of aqueous H2O2 and its mass equivalent injection of pure water. Both injections that included H_2O_2 advanced combustion with respect to the cycle with no injection. The larger H_2O_2 injection advanced combustion more and had a lower peak temperature than the smaller H_2O_2 injection. Both injections of pure water delayed combustion with respect to the cycle with no injection. The larger water injection delayed combustion more and had a lower peak temperature than the smaller water injection.

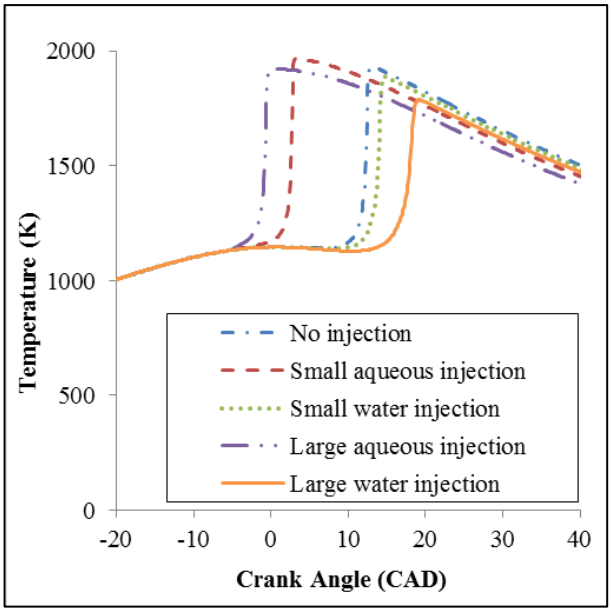

Figure 18. The effects on the temperature profile created by equivalent injections of pure water and aqueous H_2O_2 have on CA50 when SOI is -5 CAD and the intake temperature is 460 K.

The reduction in peak temperature has a beneficial influence on emissions since they are heavily dependent on temperature.[32] Figure 19 exhibits the effect of H_2O_2 concentration on the NO_x emissions. In this simulation, SOI was adjusted to achieve a CA50 of 3 $\pm$ 0.3 CAD for all trials. The simulations showed that the addition of H_2O_2 has a positive effect on the emissions of NO_x. Moreover, the addition of H_2O_2 can allow the engine to run at lower temperatures and maintain the same CA50, thereby indirectly decreasing the emissions of NO_x.

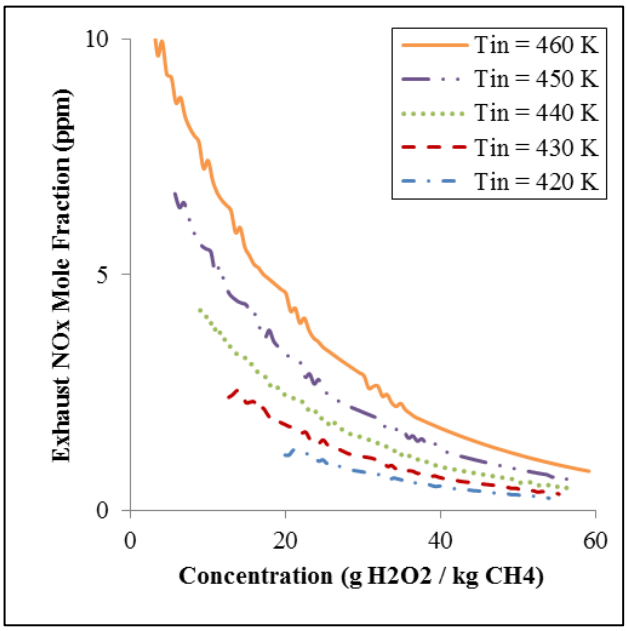

Figure 19. The relationship between the concentration of H_2O_2 and the emissions of NO_x while CA50 is held constant at 3 $\pm$ 0.3 CAD.

Furthermore, because the increased concentration of radicals promotes the decomposition of organic compounds, increasing H_2O_2 concentration increases combustion completeness. As a result, exhaust CO lessens as the H_2O_2 concentration is increased. Figure 20 shows the decreasing trend in exhaust CO mole fraction as the H_2O_2 concentration is increased. SOI was adjusted to achieve a CA50 of 3 ± 0.3 CAD for all trials. Although a single-zone model may be insufficient to gather the effects of unburned charge trapped in piston crevices[33], these emissions trends are enough to encourage further investigation.

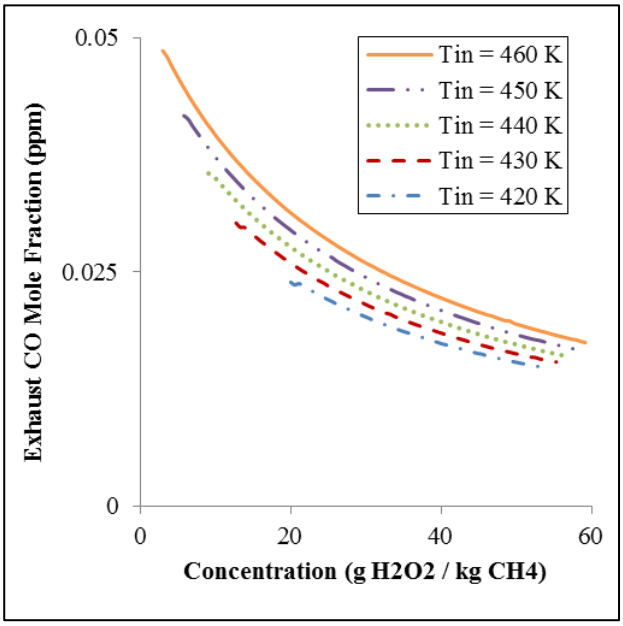

Figure 20. The relationship between the concentration of H_2O_2 and the emissions of CO while CA50 is held constant at 3 ± 0.3 CAD.

Pressure analysis was performed to calculate the indicated mean effective pressure (IMEP), the heat release rate (HRR), and the cumulative heat release (CHR). Figure 21 depicts the effect of the H_2O_2 addition on the IMEP while holding CA50 constant. As the concentration of H_2O_2 increases, IMEP tends to decrease due to the additional water present in the combustion chamber. As shown in Figures 16 and 17, the additional water decreases the peak in-cylinder pressure and temperature and thus the trend of decreasing IMEP at higher H_2O_2 concentrations.

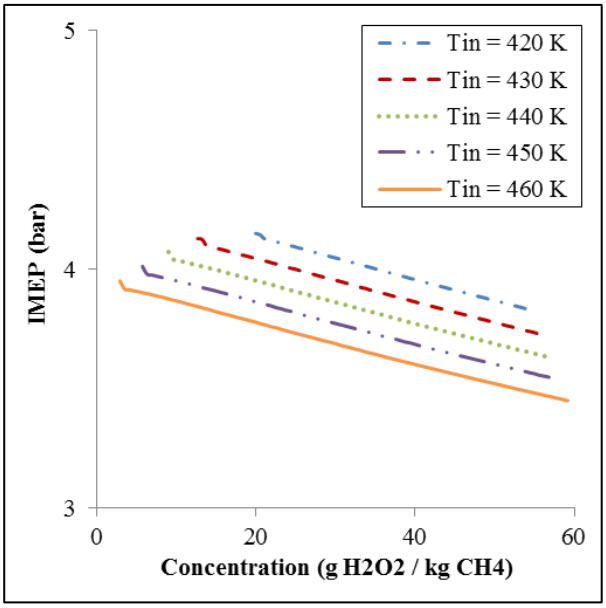

Figure 21. The effect of the concentration of H_2O_2 on IMEP. CA50 is held constant at 3 ± 0.3 CAD.

Figure 22 shows the effect of the amount of H_2O_2 addition on the HRR at an intake temperature of 460 K and a SOI of -5 CAD. As the amount of added H_2O_2 increases, the timing of the peak HRR advances with combustion timing. Similarly, Figure 23 shows the effect of SOI on the HRR at an intake temperature of 460 K and a 100 mg H_2O_2 solution injection. As the SOI is advanced, the peak HRR advances with combustion timing. Maximum HRR is achieved when combustion occurs shortly after TDC.

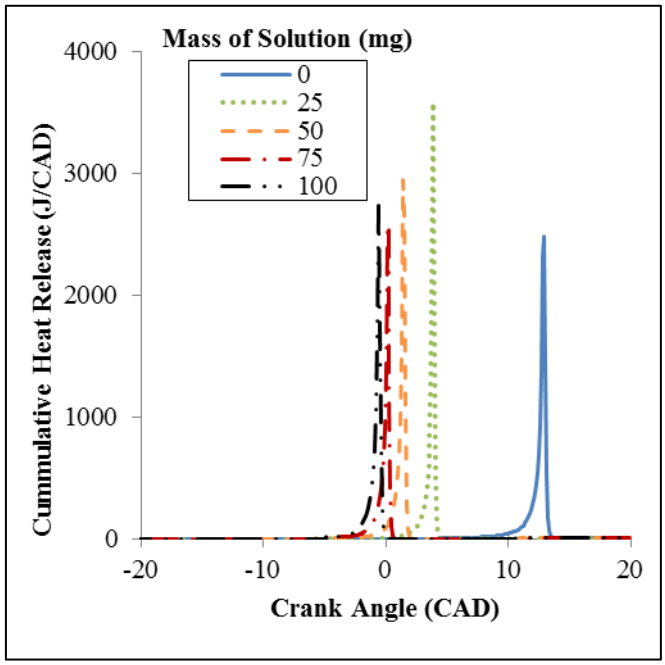

Figure 22. The effect of the amount of H_2O_2 on the heat release rate. SOI is held constant at -5 CAD and intake temperature is 460 K.

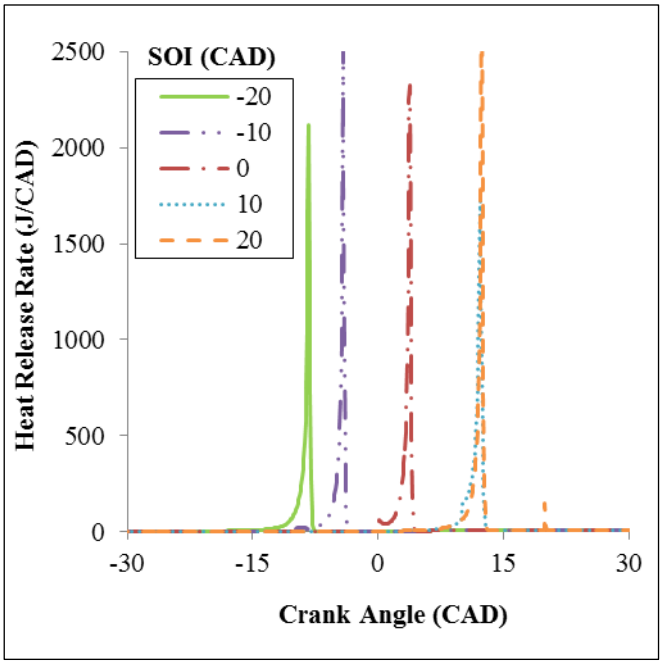

Figure 23. The effect of the SOI of 100 mg of solution on the heat release rate at an intake temperature is 460 K.

Figure 24 shows the effect of the amount of H_2O_2 addition on the CHR at an intake temperature of 460 K and a SOI of -5 CAD. As the amount of added H_2O_2 increases, the CHR decreases due to lower in-cylinder peak temperatures. Combustion did not occur when the SOI was 10 and 20 CAD. Figure 25 shows the effect of SOI on the CHR at an

intake temperature of 460 K and a 100 mg aqueous H_2O_2 injection. The CHR decreases as SOI advances due to change of the in-cylinder specific heat ratio introduced by the aqueous H_2O_2 injection.[34]

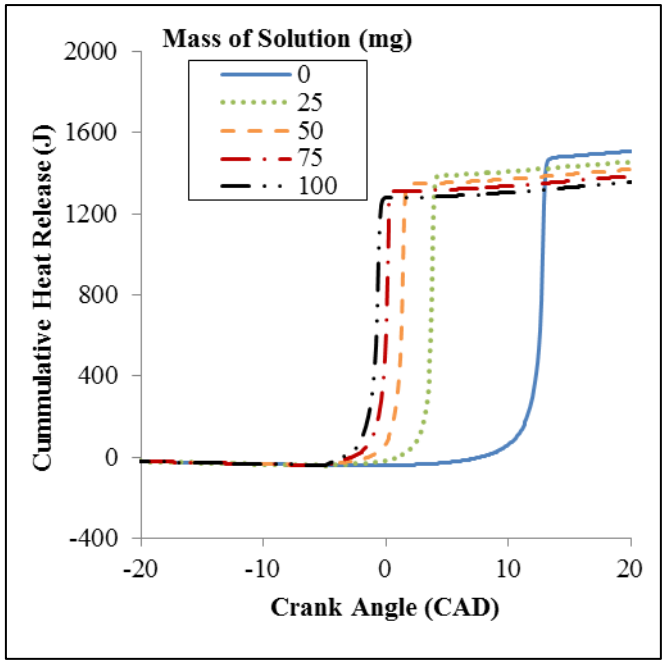

Figure 24. The effect of the amount of H_2O_2 on the cumulative heat release. SOI is held constant at -5 CAD and intake temperature is 460 K.

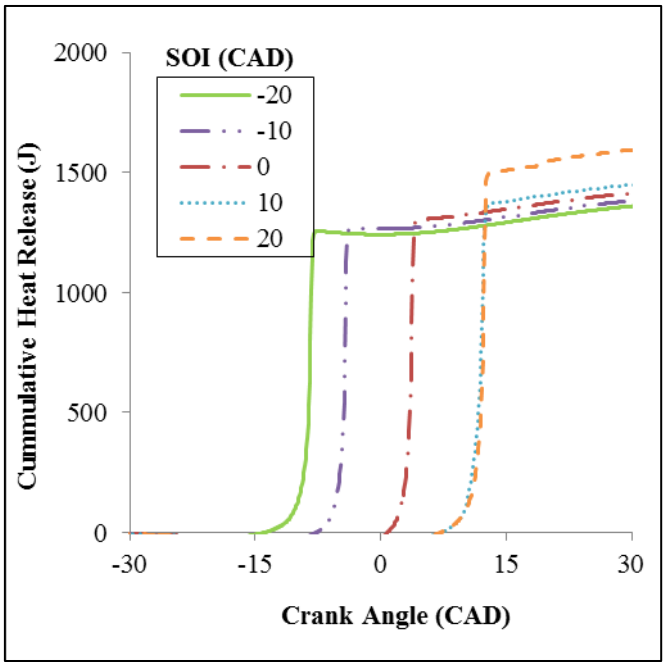

Figure 25. The effect of the SOI of 100 mg of solution on the cumulative heat release at an intake temperature is 460 K.

Conclusions

The effects of the direct injection of aqueous H_2O_2 into a methane fueled HCCI engines were investigated numerically. This study suggests that a directly injected aqueous mixture of H_2O_2 can provide the ability to control combustion phasing in HCCI engines while preserving low emissions and high efficiencies. The introduction of small quantities of H_2O_2 can effectively advance the ignition of methane. The application of direct injection of H_2O_2 has the potential to

negate some of the difficulties associated with controlling the combustion event and expand the range of combustion regimes at which HCCI operates. The manipulation of H_2O_2 concentration and SOI provides two tools which can be utilized to achieve desired combustion timing under a wide range of intake conditions. This can be achieved while maintaining low emissions and peak in-cylinder pressures.

While the results of this experiment are promising, the expansion of the computational model to multiple zones in order to capture the non-homogenous nature of the H_2O_2 injection will yield further insight into the behavior of the dual fuel combustion control strategy. Additionally, the effect of higher intake pressures on the viability of H_2O_2 addition needs to be addressed since many HCCI engines are now incorporating boosted operating conditions to increase the power density of the engine. Further investigation through experimentation or an expansion of the single-zone model into a multi-zone model is necessary to validate the strategy.

References

1 Flowers D. L., Killingsworth N. J., Espinosa-Loza F., Martinez-Frias J., Aceves S.M., Krstic M., and Dibble R. Demonstrating optimum HCCI combustion with advanced control technology. SAE Paper 2009-01-1885; 2009.

2 Strandh, P., Bengtsson, J., Johansson, R., Tunestål, P. *et al*. Cycle-to-cycle control of a dual-fuel HCCI engine. SAE Technical Paper, 2004-01-0941.

3 Martinez-Frias J., Aceves S. M., Flowers D., Smith J. R., and Dibble R. HCCI control by thermal management. SAE paper, 2000-01-2869.

4 Haraldsson, G., Tunestål, P., Johansson, B., and Hyvönen, J. HCCI closed-loop combustion control using fast thermal management. SAE Technical Paper, 2004-01-0943.

5 Erlien S. M., Jungkunz A. F. and Gerdes , C. Multicylinder HCCI control with coupled valve actuation using model predictive control. Journal of Dynamic Systems, Measurement, and Control, 2013, 135(5), 051018 .

6 Nakamura, Y., Jung, D., and Iida, N. Closed-loop combustion control of a HCCI engine with re-breathing EGR system. SAE International Journal of Engines, 6(4):2013.

7 Aldawood, A., Mosbach, S. and Kraft, M. HCCI combustion control using dual-fuel approach: experimental and modeling investigations. SAE Technical Paper, 2012-01-1117.

8 Kokjohn, S., Hanson, R., Splitter, D., and Reitz, R. Experiments and Modeling of Dual-Fuel HCCI and PCCI Combustion Using In-Cylinder Fuel Blending. SAE International Journal of Engines, 2010, 2(2), pp. 24-39.

9 Hountalas, D. and Papagiannakis, R. Theoretical and experimental investigation of a direct injection dual fuel diesel-natural gas engine. SAE Technical Paper, 2002-01-0868.

10 Mack, J. H., Buchholz, B. A., Flowers, D. L. and Dibble, R. W. The effect of the di-tertiary butyl peroxide (DTBP) additive on HCCI combustion of fuel blends of ethanol and diethyl ether. SAE Technical Paper, 2005-01-2135, 2005.

11 Huang, Z., Ji, L., Dong, H., Yang, Z. and Lu, X. Experimental study on dual-fuel compound homogeneous charge compression ignition combustion. International Journal of Engine Research, 2012.

12 Sun, X., Aia, A. and Hussain, S. A dual-fuel system for motor vehicles. SAE Technical Paper, 1998, 981356.

13 Kuwahara, K. and Ando, H. Role of heat accumulation by reaction loop initiated by H2O2 decomposition for thermal ignition. SAE Technical Paper, 2007, 2007-01-0908.

14 Mulenga, M., Ting, D., Reader, G., and Zheng, M. The potential for reducing CO and NO_x emissions from an HCCI engine using H2O2 addition. SAE Technical Paper, 2003, 2003-01-3204.

15 Noorpoor, A. R. , Ghaffarpour, M. , Aghsaee, M. and Hamedani , A. Effects of fuel additives on ignition timing of methane fuelled HCCI engine. Journal of the Energy Institute, 2009, Volume 82, Number 1, pp. 37-42.

16 Tian, L., Jun, D., Tangtang, B. and Zhijun, W. Numerical study on effect of hydrogen peroxide additive on ethanol HCCI engine, Advanced Materials Research, 2012, Volumes 433-440, pp. 244-250.

17 Christensen, M. and Johansson, B. Homogeneous charge compression ignition with water injection. SAE Technical Paper, 1999, 1999-01-0182.

18 Iwashiro, Y., Tsurushima, T., Nishijima, Y., Asaumi, Y. *et al.* Fuel consumption improvement and operation range expansion in HCCI by direct water injection. SAE Technical Paper, 2002, 2002-01-0105.

19 Mack, J. H., Aceves, S. M., and Dibble, R. W. Demonstrating direct use of wet ethanol in a homogeneous charge compression ignition (HCCI) engine, Fuel, 2006, 85, pp. 2622–2631.

20 Megaritis, A., Yap, D. and Wyszynski, M. L. Effect of inlet valve timing and water blending on bioethanol HCCI combustion using forced induction and residual gas trapping. Fuel, May 2008, Volume 87, Issue 6, pp. 732-739.

21 Carlucci, A. P., Laforgia, D., and Saracino, R. Effects of in-cylinder bulk flow and methane supply strategies on charge stratification, combustion and emissions of a dual-fuel DI diesel engine. SAE Technical Paper, 2009, No. 2009-01-0949.

22 Namasivayam, A. M., Crookes, R. J., Korakianitis, T., and Olsen, J. Assessment of combustion in natural gas dual-fuelled compression ignition engines with dimethyl ether and rapeseed methyl ester pilot ignition. International Journal of Engine Research, June 1, 2009, 10(3):165-174.
23 Kokjohn, S. L., Hanson, R. M., Splitter, D. A., and Reitz, R. D. Fuel reactivity controlled compression ignition (RCCI): a pathway to controlled high-efficiency clean combustion. Internaltional Journal of Enginer Resarch. June 22, 2011, 12(3): 209-226.
24 Occupational Safety & Health Administration, U.S. Department of Labor. Purpose and use of hazardous materials table. 10 January 2008, 49 CFR 172.101.
25 Ogawa, H., Miyamoto, N., Kaneko, N. and Ando H. Combustion control and operating range expansion in an homogeneous charge compression ignition engine with direct in-cylinder injection of reaction inhibitors. International Journal of Engine Research, August 1, 2005, 6: 341-359.
26 Goodwin, D. Cantera: an object-oriented software toolkit for chemical kinetics, thermodynamics, and transport processes, available at http://code.google.com/p/cantera/, 2013.
27 Smith, G. P., Golden, D. M., Frenklach, M., Moriarty, N. W., Eiteneer, B., Goldenberg, M., Bowman, C. T., Hanson, R. K., Song, S., Gardiner, W. C., Lissianski, V. V. and Qin, Z. GRI-Mech. http://www.me.berkeley.edu/gri_mech/
28 Stone, R. Introduction to internal combustion engines, Society of Automotive Engineers, Inc., Warrendale, PA, 1999.
29 Martinez-Frias, J., Dibble, R. W., Aceves, S. M., Flowers, D. L. and Smith, J. R. Thermal charge conditioning for optimal HCCI engine operation, J. Energy Resources Technology, March 2002, 124(1), pp. 67-75.
30 Morsy, M.H. Ignition control of methane fueled homogeneous charge compression ignition engines using additives. Fuel, 2007, 86, pp. 533–540.
31 Liu, Y., Shi, X., Deng, J., Chen, Y. *et al*. Experimental study on the characteristics of knock under DI-HCCI combustion mode with ethanol/gasoline mixed fuel. SAE Technical Paper 2013-01-0544; 2013.
32 Abdelghaffar, W.A. NOx formation inside HCCI engines. American Journal of Scientific and Industrial Research, 2010.
33 Chin, G., and Chen, J. Y. Modeling of emissions from HCCI engines using a consistent 3-zone model with applications to validation of reduced chemistry. Proceedings of Combustion Institute, 33, Issue 2, 2011, pp. 3073-3079.
34 Chun, K. M., and Heywood, J. B. Estimating heat-release and mass-of-mixture burned from spark-ignition engine pressure data. Combustion Science and Technology, 1987, 54(1-6), 133-143.

Abbreviations

ATDC	after top dead center
BDC	bottom dead center
CAD	crank angle degree
CAT	Caterpillar
CHR	cumulative heat release
HCCI	homogeneous charge compression ignition
HRR	heat release rate
IMEP	indicated mean effective pressure
SOI	start of injection
TDC	top dead center